MULTI-SPECTRAL WIDEFIELD MICROSCOPY OF THE BEATING HEART THROUGH POST-ACQUISITION SYNCHRONIZATION AND UNMIXING

Christian Jaques[⋆†◇] *Linda Bapst-Wicht*[*] *Daniel F. Schorderet*[*†] *Michael Liebling*[⋆‡]

[⋆] Idiap Research Institute, CH-1920 Martigny, Switzerland
[†] École Polytechnique Fédérale de Lausanne, CH-1015 Lausanne, Switzerland
[*] Institut de Recherche en Opthalmologie, CH-1950 Sion, Switzerland
[‡] Electrical and Computer Engineering, University of California, Santa Barbara, CA 93601, USA
[◇]christian.jaques@idiap.ch

ABSTRACT

Multi-spectral imaging allows distinguishing biological structures. For cardiac microscopy, available devices are either too slow or require illumination intensities that are detrimental to the sample. We present a method for spectral super-resolution imaging of samples whose motion is quasi-periodic by sequentially acquiring movies in wavelength ranges with filters of overlapping bands. Following an initial calibration procedure, we synchronize and unmix the movies to produce multi-spectral sequences. We characterized our approach to retrieve the transmittance of a colored microscopic target whose motion we controlled, observing measurements within of 10% that of a reference spectrometer. We further illustrate our approach to observe the beating embryonic zebrafish heart, demonstrating new possibilities for studying its development.

***Index Terms*—** Microscopy, spectral imaging, time registration, inverse-problems, cardiac imaging

1. INTRODUCTION

Live cardiac imaging in the developing heart is a complex task as the heart beats while it develops and illumination must be limited to prevent damage to the sample. Multi-spectral imaging could benefit the study and differentiation of cardiac structures but as the available light is limited, multi-spectral imagers require operation times that are too slow for cardiac applications.

We propose a method to perform multi-spectral imaging of the beating heart by acquiring a set of movies of the beating heart over multiple heartbeats, each recording a signal filtered in different (and possibly overlapping) range of wavelengths. From these multi-channel data, we build a single multi-spectral movie of the beating heart through temporal registration of the movies followed by color unmixing to yield non-overlapping wavelength ranges (Fig. 1).

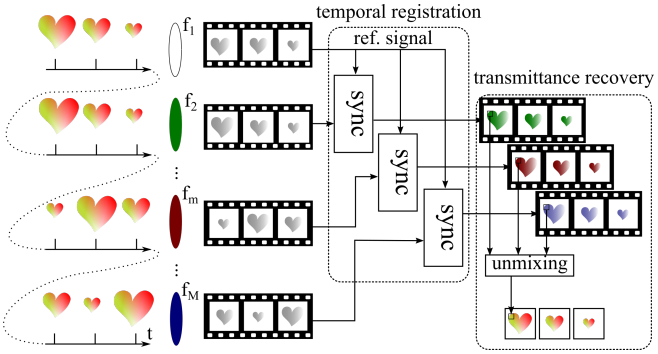

Fig. 1. Overview of the method: (1) we acquire M movies of a live beating heart with M different filters, where the first filter is an all-pass that serves as registration reference; (2) we register all acquired movies to the reference sequence; (3) we perform unmixing pixel-by-pixel in order to retrieve a multi-spectral movie of the beating heart.

The importance of multi-spectral imaging in wide-field (non-fluorescence) microscopy and biomedical imaging has been identified in the past. Aach et al. [1] detected cancerous cells through spectral imaging. Blasinski et al. [2] have shown that spectral imaging improves the classification accuracy of ablated heart tissue using machine learning.

Spectral cameras typically acquire multiple images sequentially with narrow-band filters or split the incoming light onto multiple sensors, based on the wavelength [3]. While the first solution makes the imaging process slow, hence unsuitable to image dynamic sample, the second solution trades spatial resolution or signal intensity for spectral resolution. Also, building such cameras requires high opto-mechanical precision and little flexibility for the end user to adjust to particular wavelength ranges.

This work is supported by projects funded by the Swiss National Science Foundation (SNSF), grants 200021_159227 "Computational Methods for Temporal Super-resolution Microscopy", Grant 200020_179217 "Computational biomicroscopy: advanced image processing methods to quantify live biological systems", and Grant 206021_164022 "Platform for Reproducible Acquisition, Processing, and Sharing of Dynamic, Multi-Modal Data."

To overcome these limitations, methods to achieve spectral imaging through computational approaches with less constraining hardware have been proposed. For example, multiple observations of the same scene, observed through a set of colored filters are combined to reconstruct a multi-spectral view [4, 5, 6]. Other approaches have considered spectral imaging as an interpolation or a learning process, using priors on the signal to be reconstructed [7, 8, 9].

Here, we build upon the former class of methods (direct unmixing) that we combine with the multi-channel synchronization step described in Ohn et al. [10] for cardiac imaging of multiple fluorescence channels imaged one after the other, with a brightfield movie as the common reference to synchronize movies collected in 6 bands.

The contributions of this work are (i) presentation of a pipeline to sequentially collect and process multi-spectral images of the beating heart (described in Sections 2 and 3), (ii) characterization of the proposed approach on a controlled dynamic microscopy sample (Section 4) and (iii) demonstration of the applicability for imaging the beating heart of a zebrafish (Section 4.2). We discuss results and conclude in Section 5.

2. PROBLEM STATEMENT

We consider a multispectral, T-periodic signal s such that:

$$s(\boldsymbol{x}, \lambda, t) = s(\boldsymbol{x}, \lambda, t + T), \quad \text{for all time } t \in \mathbb{R}, \tag{1}$$

where $\boldsymbol{x} = (x_1, x_2)$ are spatial coordinates and λ the wavelength. The signal s represents the transmissivity of a sample to incoming light over time. We further consider M movies:

$$y_m[\boldsymbol{k}, \ell] = \sum_{\lambda_1, \ldots, \lambda_N} a_m[\lambda_n] s(\boldsymbol{k}\Delta x, \lambda_n, \ell\Delta t + \tau_m) + c, \tag{2}$$

with pixels indexed by $\boldsymbol{k} = (k_1, k_2) \in \mathcal{K} = \{0, \ldots K_1\} \times \{0, \ldots K_2\}$, frames indexed by $0 \leq \ell < L$, Δx and Δt the sampling steps in space and time, respectively. The factors a_m incorporate the combined effect of illumination source, bandpass filters (indexed by $m \in \{1, \ldots, M\}$), and the spectral response and gain of the camera. c is a scalar offset of the camera and τ_m is a delay that describes the fact that we acquire movies with different filters in different cardiac cycles, starting at an arbitrary (non-triggered and unknown) cardiac phase. We further assume that the movie duration covers at least a full heartbeat, i.e., we have $L > T/\Delta t$.

The problem we address is to determine an estimate $\tilde{s}$ of the multi-spectral transmission function of the sample s such that $\tilde{s}[\boldsymbol{k}, \lambda_n, \ell] \approx s(\boldsymbol{k}\Delta x, \lambda_n, \ell\Delta t)$, for $\boldsymbol{k} \in \mathcal{K}$, $\lambda_n \in \{\lambda_1, \ldots, \lambda_N\}$ and $0 \leq \ell < \lfloor T/\Delta t \rfloor$ given the M movies $y_m[\boldsymbol{k}, \ell]$ in Equ. (2).

3. METHODS

Our methods cover the determination of the unknown time-delays between channel acquisitions ($\tau_m > T$), spectral unmixing to invert Equ. (2), and a calibration procedure to determine the factors $a_m[\lambda_n]$.

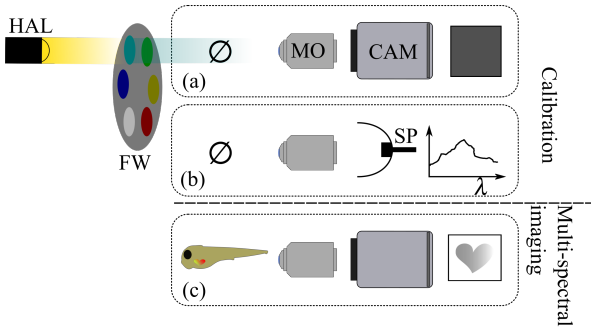

Fig. 2. Setup for the acquisition of data; MO: microscope objective, HAL: halogen lamp, CAM: camera, SP: spectrometer, FW: filter wheel. For the calibration, we both use (a) a camera or (b) a spectrometer at the measuring end of the setup, with no setup. After calibration, the system may be used for spectral imaging with dynamic samples (c).

3.1. Temporal registration of movies acquired with different filters

Since we collect the spectral response (channels) in different cardiac cycles without any caring signal, before we can merge the channels to obtain the spectral transmission we first need to temporally synchronize the movies.

We proceed to the registration using a method described before by Liebling et al. [11] and, in particular, Ohn et al. [12, 10] for the problem of synchronizing microscopy image series of the beating heart imaged of differing contrasts. Briefly, for each of the M movies y_m corresponding to the M channels, the method determines the shifts τ_m such that the P frames that we aim to reconstruct (and which cover a cardiac heartbeat) maximize the normalized mutual information between the movie of the channel to be registered, shifted by a candidate shift, and the reference channel (which we take to be a movie acquired using a broadband illumination):

$$\tilde{\tau}_m = \arg\min_{\tau} \sum_{\ell=1}^{P} \mathrm{NMI}(y_m[\cdot, \ell - \tau/\Delta t], y_0[\cdot, \ell]), \tag{3}$$

where $\mathrm{NMI}(a, b)$ is the normalized mutual information [13, 12] between two images. After we determine the estimates $\tilde{\tau}_m$, $1 \leq m \leq M$, we apply them to obtain synchronized movies $\tilde{y}_m[\boldsymbol{k}, \ell] = y_m[\boldsymbol{k}, \ell - \tilde{\tau}_m/\Delta t]$, $\boldsymbol{k} \in \mathcal{K}$ and $0 \leq \ell < P$.

3.2. Spectral imaging/unmixing

Given synchronized movies in M channels, we can consider the spectral recovery problem as a point-wise problem and we drop the spatial ($\boldsymbol{k}$) and temporal (ℓ) dependency for brevity. Our aim is to reconstruct a discrete transmission spectrum $\boldsymbol{s} = \big(s_{\lambda_1}, \ldots, s_{\lambda_N}\big)^\top = \big(s(\lambda_1), \ldots, s(\lambda_N)\big)^\top$. We start by describing the acquisition model in more detail, considering our imaging system that consists of a monochrome camera, an illumination source, and M interchangeable filters (Fig. 2). Combining the effect of the wavelength-dependent

light source emission intensity e_{λ_n}, transmissivity f_{m,λ_n} of the m^{th} filter and the spectral response g_{λ_n} of the camera, the measured intensity at a pixel is:

$$y_m = c + \sum_{\lambda_1,\ldots,\lambda_N} \underbrace{g_{\lambda_n} e_{\lambda_n} f_{m,\lambda_n}}_{a_m[\lambda_n]} s_{\lambda_n}, \tag{4}$$

where we identified the factors $a_m[\lambda_n]$ of Equ. (2). In matrix form, with $\boldsymbol{y} = (y_1, \ldots, y_M)^\top$, we can write:

$$\boldsymbol{y} = \boldsymbol{FGs} + \boldsymbol{c}, \tag{5}$$

with

$$\boldsymbol{F} = \begin{pmatrix} f_{1,\lambda_1} e_{\lambda_1} & \cdots & f_{1,\lambda_N} e_{\lambda_N} \\ \vdots & \ddots & \vdots \\ f_{M,\lambda_1} e_{\lambda_1} & \cdots & f_{M,\lambda_N} e_{\lambda_N} \end{pmatrix}, \tag{6}$$

$\boldsymbol{G} = \text{diag}(g_{\lambda_1}, \ldots, g_{\lambda_N})$, $\boldsymbol{c} = c\mathbf{1}_{M\times 1}$. With these notations, we formulate the problem of retrieving an estimate of the spectral transmittance $\tilde{\boldsymbol{s}}$ of the sample can be formulated as the solution to a minimization problem:

$$\tilde{\boldsymbol{s}} = \arg\min_{\boldsymbol{s}} \|\boldsymbol{y} - \boldsymbol{c} - \boldsymbol{As}\|_{\ell_1} \tag{7}$$

where $\boldsymbol{A} = \boldsymbol{FG}$. We solve this problem using a simplex method [14] with the additional constraints that $0 \leq \tilde{\boldsymbol{s}} \leq 1$.

3.3. Calibration of the imaging system

Before solving Equation (7), we must calibrate the system to populate matrices $\boldsymbol{F}$ and $\boldsymbol{G}$. We use a spectrometer to directly measure the combined spectral response of each filter with the light source spectrum (Fig. 2 (b)) and populate the M rows of $\boldsymbol{F}$. To calibrate $\boldsymbol{G}$, we place the camera in the acquisition setup (Fig 2 (a)) and sequentially acquire M images with an empty sample holder ($s_{\lambda_n} = 1$ in Equation (4)):

$$\begin{aligned} \underbrace{\begin{pmatrix} y_{1,\text{cal}} \\ \vdots \\ y_{M,\text{cal}} \end{pmatrix}}_{\boldsymbol{y}_{\text{cal}}} &= \begin{pmatrix} \boldsymbol{F} & \mathbf{1}_{M\times 1} \end{pmatrix} \text{diag}(g_{\lambda_1}, \ldots, g_{\lambda_N}, c)\mathbf{1}_{N\times 1} \\ &= \begin{pmatrix} \boldsymbol{F} & \mathbf{1}_{M\times 1} \end{pmatrix} \big(\underbrace{g_{\lambda_1} \quad \ldots \quad g_{\lambda_N} \quad c}_{\boldsymbol{g}_{\text{cal}}} \big)^\top. \end{aligned} \tag{8}$$

To retrieve $\boldsymbol{g}^\star_{\text{cal}}$, we solve (with constraint $0 \leq \boldsymbol{g}^\star_{\text{cal}} \leq 1$):

$$\boldsymbol{g}^\star_{\text{cal}} = \arg\min_{\boldsymbol{g}} \left\| \boldsymbol{y}_{\text{cal}} - \begin{pmatrix} \boldsymbol{F} & \mathbf{1}_{M\times 1} \end{pmatrix} \boldsymbol{g} \right\|_{\ell_1}. \tag{9}$$

4. RESULTS

We used the transmission line of an OpenSPIM microscope [15], equipped with a condenser and illuminator (Fig. 2). We used a halogen light source (Decostar, Osram), a band-pass filter set (*FKB-VIS-40*, Thorlabs) with 5 filters (*FB500-40*, *FB550-40*, *FB600-40*, *FB650-40*, *FB700-40*, Thorlabs) mounted on a 6-position filter wheel (*FW102CNEB*, Thorlabs). The sample was held by a four dimensional stage (*USB 4D-STAGE*, Picard). We used a 20×/0.5 water immersion microscopy lens (*UMPLFLN 20xW*, Olympus) coupled to a 180 mm tube-lens (*U-TLU-1-2*, Olympus), a 4Mpixels CMOS camera (*Zyla 4.2 sCMOS*, Andor, Oxford Instruments) and a single pixel CCD spectrometer (*CCS100*, Thorlabs).

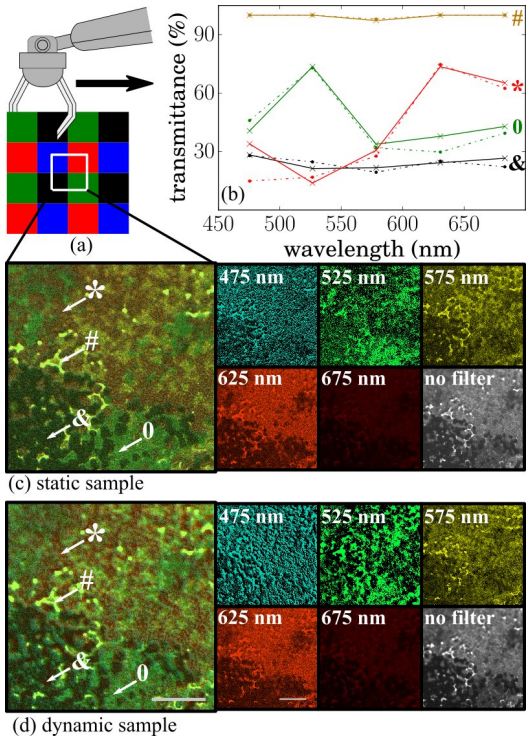

Fig. 3. Experimental validation. (a) color target mounted on a motorized sample holder. (b) Spectral transmission calculated in four points from static (solid curve) and dynamic data (dashed curve). (c)-(d) RGB-colorized reconstruction, five unmixed wavelength ranges, and acquired bright-field image in (c) static case and (d) dynamic case. Scale bars are 50 μm.

4.1. Experimental validation

Static validation: We evaluated the performance of our multi-spectral imaging method by placing color filters (*E009, E010, E022, E036, E053, E075* filters, *E-colors* set, Rosco Laboratories) in the sample holder and comparing the recovered spectra with those measured directly with the spectrometer. We observed a median error of around 10%.

Dynamic validation: we laser-printed a color pattern on a transparency that we mounted on the sample holder (Fig. 3(a)). We first reconstructed the transmittance from measurements carried out with the sample at rest (Fig. 3(c)). Next, we collected movies of the target displaced laterally with the positioning stage of the microscope, repeating the same motion for each filter, hence generating a pseudo-periodic signal (Fig. 3(d)). The recovered spectra in the static and dynamic case concur (Fig. 3(b)).

4.2. Spectral imaging of the beating heart of a zebrafish

To illustrate the potential of our method in practice, we image the heart of a live zebrafish larva. All experiments were approved by the Veterinary service of the State of Valais (Switzerland). We raised and kept zebrafish (wild-type AB zebrafish strain (Zebrafish International Resource Center)

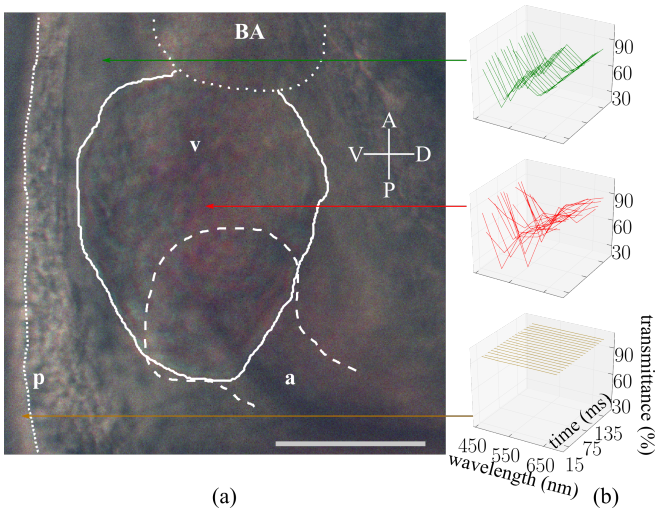

Fig. 4. (a) Color rendering of the reconstructed multi-spectral zebrafish heart. The atrium (a), ventricle (v), bulbus arteriosus (BA), and pericardium (p) are outlined. (b) Spectral transmittance computed at times covering a full cardiac period. Scale bar is 100 μm. See also supplementary video.

under standard laboratory conditions (14/10 hour light/dark cycle, fish water of the system (ZEBTEC Techniplast Aquatic Solution) at 26.5°C temperature, 500 μs conductivity, and pH 7.3). We raised embryos at 29°C in standard E3 medium in an incubator (Termaks B8054), supplemented by 0.003% 1-phenyl 2-thiourea (PTU) from 24 hours post fertilization (hpf) to prevent pigmentation. For imaging, we embedded 48 hpf larvae (hatched from chorion), anesthetized with 0.1% tricaine (ethyl 3-aminobenzoate methanesulfonate salt, Sigma), in low melting agarose for imaging until aged 5 days post fertilization at most. We reconstructed both a color movie and transmittance spectra in multiple areas of the heart (Fig. 4) clearly showing spectral variations (background, red blood cells, cardiac tissue).

5. DISCUSSION AND CONCLUSION

We observed median errors on the recovery of transmittance data around 10%, with averages around 30% due to higher errors at low wavelength ranges where the illumination source provides insufficient intensity. In addition to images with high signal-to-noise (which requires illumination of consistent intensity in all wavelength ranges), for Equations (8) and (9) to be well-posed we must have $N + 1 \leq M$ (we must have at least one more filter than wavelength range to be recovered) and the filter band should be such that $\boldsymbol{F}$ has high rank (small overlap between filters). A critical point of the method is the temporal registration of the acquired movies. Poorly synchronized movies lead to worse spectral recovery. In conclusion, we presented and characterized a practical method to perform dynamic multi-spectral microscopy of samples with periodic motion. Results from the beating heart of a zebrafish larva show the potential applicability for studying cardiac dynamics and differentiating tissues and cells.

6. REFERENCES

[1] A. A. Bell, J. Brauers, J. N. Kaftan, D. Meyer-Ebrecht, A. Böcking, and T. Aach, "High dynamic range microscopy for cytopathological cancer diagnosis," *IEEE J. Sel. Topics Signal Process.*, vol. 3, no. 1, pp. 170–184, 2009.

[2] H. Blasinski, J. Farrell, B. Wandell, and P. Wang, "Multispectral imaging of tissue ablation," *Proc. IEEE Int. Symp. Biomed. Imag.*, pp. 360–363, 2016.

[3] N. Gat, "Imaging spectroscopy using tunable filters: a review," *Proc. SPIE Wavelet Application VII*, vol. 4056, pp. 50–64, 2000.

[4] J. I. Park, M. H. Lee, M. D. Grossberg, and S. K. Nayar, "Multispectral imaging using multiplexed illumination," in *Proc. IEEE Int. Conf. on Comput. Vis.*, 2007, pp. 1–8.

[5] C. Chi, H. Yoo, and M. Ben-Ezra, "Multi-spectral imaging by optimized wide band illumination," *Int. J. Comput. Vis.*, vol. 86, no. 2-3, pp. 140–151, 2010.

[6] S. W. Oh, M. S. Brown, M. Pollefeys, and S. J. Kim, "Do it yourself hyperspectral imaging with everyday digital cameras," *Proc. IEEE Conf. on Comput. Vis. and Pat. Recog.*, pp. 2461–2469, 2016.

[7] S. Galliani, C. Lanaras, D. Marmanis, E. Baltsavias, and K. Schindler, "Learned spectral super-resolution," *Proc. IEEE Int. Conf. on Comput. Vis.*, 2017.

[8] Y. Qu, H. Qi, and C. Kwan, "Unsupervised sparse dirichlet-net for hyperspectral image super-resolution," *Proc. IEEE Conf. on Comput. Vis. and Pat. Recog.*, pp. 2511–2520, 2018.

[9] T. H. Tsai, P. Llull, X. Yuan, L. Carin, and D. J. Brady, "Spectral-temporal compressive imaging," *Opt. Lett.*, vol. 40, no. 17, pp. 4054–4057, 2015.

[10] J. Ohn, J. Yang, S. E. Fraser, R. Lansford, and M. Liebling, "High-speed multicolor microscopy of repeating dynamic processes," *Genesis*, vol. 49, no. 7, pp. 514–521, 2011.

[11] M. Liebling, J. Vermot, A. S. Forouhar, M. Gharib, M. E. Dickinson, and S. E. Fraser, "Nonuniform temporal alignment of slice sequences for four-dimensional imaging of cyclically deforming embryonic structures," *Proc. IEEE Int. Symp. Biomed. Imag.*, pp. 1156–1159, 2006.

[12] M. Liebling and H. Ranganathan, "Wavelet domain mutual information synchronization of multimodal cardiac microscopy image sequences," in *Proc. SPIE 7446*, 2009, pp. 744602 1–5.

[13] C. Studholme, D. J. Hawkes, and D. L. G. Hill, "Normalized entropy measure for multimodality image alignment," in *Proc. SPIE 3338*, 1998, pp. 132–143.

[14] G. B. Dantzig, A. Orden, and P. Wolfe, "The generalized simplex method for minimizing a linear form under linear inequality restraints," *Pac. J. Math.*, vol. 5, no. 2, pp. 183–195, 1955.

[15] P. G. Pitrone, J. Schindelin, L. Stuyvenberg, S. Preibisch, M. Weber, K. W. Eliceiri, J. Huisken, and P. Tomancak, "Openspim: an open-access light-sheet microscopy platform," *Nat. Meth.*, vol. 10, no. 7, pp. 598–599, jul 2013.